Real-Time Evolution of the Valence Electronic Structure in a Dissociating Molecule

Ph. Wernet,[1,*] M. Odelius,[2] K. Godehusen,[1] J. Gaudin,[1,†] O. Schwarzkopf,[1] and W. Eberhardt[1]

[1]*Helmholtz-Zentrum Berlin, Albert-Einstein-Strasse 15, D-12489 Berlin, Germany*

[2]*FYSIKUM, Stockholm University, AlbaNova, S-106 91 Stockholm, Sweden*

(Received 30 January 2009; published 29 June 2009)

Time-resolved valence band photoelectron spectroscopy with a temporal resolution of 135 fs is used to map the entire occupied valence electronic structure of photoexcited gas-phase Br_2 molecules during dissociation. The observed shifting and mixing of valence energy levels defines a transition period where the system appears to be intermediate between atoms and molecules. The surprisingly short bond breaking or dissociation time is determined by monitoring in real time how the photoelectron multiplet structure of the free atom arises from the valence states of the photoexcited molecule.

DOI: 10.1103/PhysRevLett.103.013001 PACS numbers: 32.80.Fb, 33.60.+q, 42.65.Ky, 82.53.Eb

Femtosecond x-ray pulses have recently become available with sufficiently short pulse duration and high flux to directly map the dynamics of nuclei on their intrinsic time scale of femtoseconds (fs) with ultrafast x-ray diffraction [1–3]. As nuclei move during ultrafast processes the electrons making the bonds move concomitantly entailing fs changes of the electronic structure. Such changes have been exploited with spectroscopic methods using fs photon sources from the vacuum-ultraviolet (VUV) to the hard x-ray energy region to elucidate chemical reactions in solution [4], atomic and molecular dynamics in the gas phase [5–10], on surfaces [11–13] and during phase transitions in solids [14–16]. Very few studies, however, have aimed at explicitly mapping the evolution of the electronic structure in order to complement the insight from mapping the nuclear dynamics and to get a complete picture. Mapping both transient electronic structure and nuclear dynamics holds the key to explaining bonding in transition states during chemical reactions and, in general, it promises unprecedented insight into the coupled motion of electrons and nuclei during ultrafast processes [17,18].

Probably the most obvious case for studying the concomitant evolution of electronic and geometric structures is the dissociation of a homonuclear diatomic molecule in the gas phase. The pioneering investigations by Nugent-Glandorf *et al.* [5,6] and Strasser *et al.* [7] represent the first and only attempt so far to map the electronic structure of a neutral molecule during dissociation. Time-resolved pump-probe photoelectron spectroscopy was used with VUV-probe pulses (duration 250–300 fs, FWHM) to detect atomic Br signals in the valence band photoelectron spectrum of gas-phase Br_2. In this Letter we address the same problem with the same method, but our considerably shorter VUV pulses (120 fs FWHM), enhanced sensitivity, and electronic structure calculations allowed us, for the first time, to map in real time the evolution of the entire occupied valence electronic structure of a dissociating neutral molecule. We demonstrate how probing the electronic structure complements probing the nuclear dynamics and how this allows for unprecedented insight into the dissociation of a molecule.

The Br_2 molecules were excited by single-photon absorption at 395 nm (frequency-doubled fundamental of 790 nm, pulse duration 60 fs FWHM). This entails electronic excitation to the Br_2^* ($^1\Pi_u$) dissociative state [19] and dissociation results in two ground-state Br atoms [5–7,20]. Pump-pulse energies amounted up to 30 μJ with a corresponding power density of less than 10^{12} W/cm^2 which is less than in [5,6] and similar to [7]. The molecules were ionized after a well-defined variable fs time delay by VUV-probe pulses from high-order harmonic generation by focusing 1 mJ of the fundamental laser beam into a Xe gas cell [21]. The 15th harmonic was selected with a grating monochromator (photon energy 23.5 eV, pulse duration 120 fs [22], overall pump-probe time resolution 135 ± 5 fs, all uncertainties correspond to one standard error, flux 5×10^9 photons/s at 1 kHz repetition rate). The photoelectron energies were analyzed with a magnetic bottle-type time-of-flight spectrometer (for details see [23]). The calculated spectra are based on the calculated electronic structure of an ensemble of Br_2 molecules during dissociation. Classical molecular dynamics (MD) simulations provided distributions of nuclear distances versus time delay. Binding energies and photoelectron intensities were calculated in fs steps from the excited molecule to the free atom. Both the MD and spectrum simulations are based on precalculated energy surfaces from relativistic multiconfigurational self-consistent-field calculations including electron correlation (CASPT2 level) and spin-orbit coupling [24] (for details see [23]).

Photoelectron spectra at selected pump-probe time delays are depicted in Fig. 1. Transient signals (-17 and 50 fs) and atomic lines ($+333$ fs) in the raw data already show that the evolution of the electronic structure is different in the ^3P and $^1D/^1S$ binding energy regions: While for ^3P a broad transient intensity distribution is already present at -17 fs where pump and probe pulses already overlap, considerable intensity has developed for ^1D and ^1S after

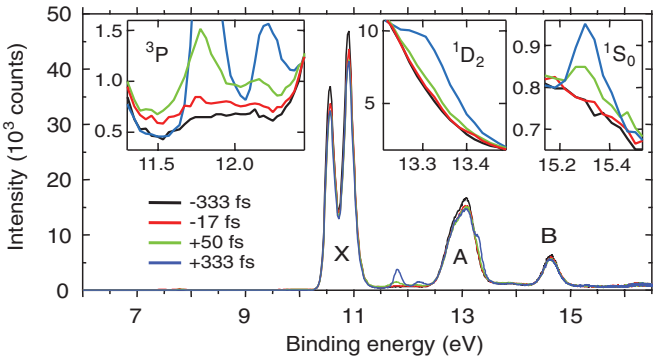

FIG. 1 (color). Photoelectron spectra at indicated delays. Main lines X, A, B: Photoionization of ground-state molecules with corresponding final ionic states Br_2^+ $^2\Pi_{g\frac{3}{2},\frac{1}{2}}$, $^2\Pi_{u\frac{3}{2},\frac{1}{2}}$, and $^2\Sigma_g$, respectively. Insets: Transient and atomic signals. Atomic lines arise from photoionization of free atoms with final ionic states Br^+ $4s^24p^4$ ($^3P_{2,1,0}$, ^1D, ^1S) [27]. Negative (positive) delays correspond to probe before (after) pump pulses. The −333 fs spectrum serves as a reference spectrum for ground-state molecules including all effects not depending on laser-induced dynamics.

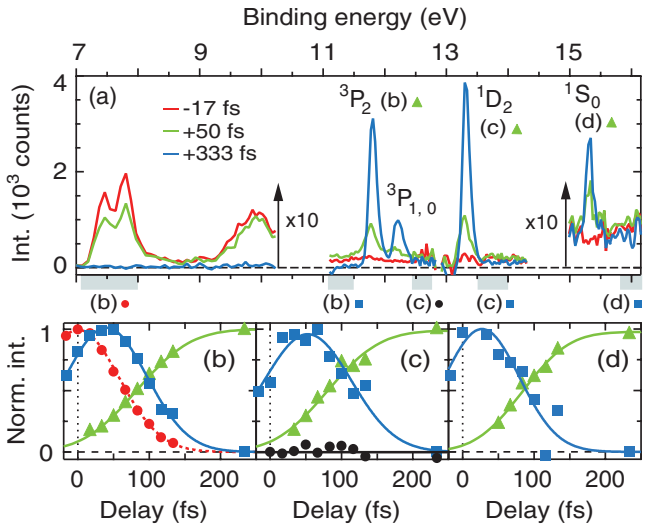

FIG. 2 (color). (a) Difference spectra at indicated delays: Sidebands at 7–10 eV, transients and atomic peaks at 11–16 eV (spin-orbit splitting in $^3P_{1,0}$ not resolved). (b)–(d) Population dynamics, i.e., photoelectron intensities versus delay. (b) Circles: Integrated sideband intensities (integration interval 7.1–8.0 eV abbreviated as 7.55 ± 0.45 eV and indicated by gray box) with Gaussian fit (dotted line, FWHM = 135 ± 5 fs). (b)–(d) Squares: Integrated intensities at (b) 11.3 ± 0.2 eV, (c) 13.75 ± 0.25 eV, (d) 16.0 ± 0.2 eV with Gaussian fits (lines) centered at (FWHM in brackets) (b) 39 ± 1 fs (135 ± 4 fs), (c) 52 ± 4 fs (144 ± 13 fs), (d) 26 ± 6 fs (124 ± 16 fs). (c) Circles: Intensities at 12.55 ± 0.15 eV. All integration intervals are indicated by gray boxes. (b)–(d) Triangles: Atomic intensities (b) $^3P_2$, (c) $^1D_2$, (d) $^1S_0$ with fitted broadened step functions (lines).

50 fs only. For a more detailed insight, the contributions to the spectrum of transients and free atoms need to be separated from the remaining intensity of ground-state molecules. This can be done by subtracting the reference spectrum (−333 fs) from the spectra at respective delays. However, since the spectrum of ground-state molecules varies with delay time (it depletes by up to 10% and shifts by up to 8 meV), a scaled and shifted reference spectrum has to be subtracted with a different scaling and shift for each delay (the shift is an ac Stark shift). How to scale and shift the reference spectrum was determined for each delay separately with measured data as shown in [23].

The resulting difference spectra for selected delays are shown in Fig. 2(a). The sidebands at 7–10 eV arise from simultaneous absorption of one VUV-probe and one laser-pump photon [10,25]. They partially obscure the observation of some of the transient features, but since they directly scale with the temporal overlap of pump and probe pulses [25] we use them to determine delay time zero and the temporal resolution of our experiment [Fig. 2(b), circles]. We find that when decreasing the pump-laser power both the sideband intensity and the shift of the spectrum of ground-state molecules decrease linearly along with the linearly decreasing atomic intensities [23]. Contrary to what was suggested in [7], this indicates that it is impossible to find pump-laser fluences where one or both of these parasitic effects can be suppressed or minimized for better detection of transient signals.

The difference spectra in Fig. 2(a) reveal important insights into the evolution of the electronic structure. Intensities just below the ^3P lines increase up to ∼50 fs and decrease hereafter while they remain approximately constant just above the ^3P lines. This can be quantified more accurately by plotting integrated intensities versus delay (population dynamics) for the respective energy regions. In addition, this analysis reveals the population dynamics for very weak intensity modulations such as above the ^1D and ^1S peaks as shown in Figs. 2(b)–2(d) (squares and Gaussian fits). Below ^3P and above ^1D and ^1S intensity increases up to a certain delay and decreases hereafter. For consistency we show that intensities remain constant at other energies [circles in Fig. 2(c)]. Apparently, intensity is shoveled with time from below ^3P and from above $^1D/^1S$ to the respective atomic peaks. This can be interpreted in a straightforward manner: During dissociation the valence state binding energies evolve from their values in the excited molecule at ground-state geometry through transient values at elongated bond distances to their final values in the free atom. Transient states are hence expected to move through the spectrum, and the observed intensity modulations directly result from states shifting from lower binding energies to the atomic ^3P and from higher energies to the $^1D/^1S$ peaks. However, we find that transient state intensities are too weak and the states shift too fast to be detected explicitly as peaks. Instead, they can be localized in time and energy by determining the time delay of maximum intensity at a particular binding energy as described above (e.g., 39 ± 1 fs for 11.3 ± 0.2 eV). These delay-energy pairs indicate the time after

excitation when the corresponding transient state has reached a certain binding energy and we place them in a map which depicts how all valence states evolve from the excited molecule to the free atom in Fig. 3(a).

We now turn to a discussion of the atomic population dynamics and come back to the delay-versus-energy map later. To separate the intensity contribution from the atomic peaks in the photoelectron spectra of Fig. 2 from that due to the transient states at a given delay, we subtracted a constant baseline representing the transient contribution from a Gaussian fit to each of the atomic peaks at that delay [23]. The centers of the Gaussians determine the atomic binding energies at the respective delay and these delay-energy pairs were added to the map in Fig. 3(a). The Gaussian intensities reflect the atomic intensities and directly correspond to the atomic population dynamics [Figs. 2(b)–2(d), triangles]. They were fit with broadened step functions (convolution of a step function with a Gaussian profile [5,6]) and the fitted steps are identical within error bars for the three final ionic states (82 ± 3 fs for ^3P, 80 ± 5 fs for ^1D, 83 ± 3 fs for ^1S). These steps directly clock the completion of the electronic structure of the free atom. Accounting for the additional uncertainty introduced by the temporal resolution [26] we find that it takes 85 ± 15 fs for the electronic structure of the free Br atom to evolve. This represents an unprecedented and unambiguous way of determining the bond breaking or dissociation time as based on the evolution of the entire valence electronic structure. Note that when fitting the total integrated intensity in the ^3P region as done in [5–7] we find the step at 45 ± 1 fs [23]. This does not correspond to the correct dissociation time because transient and atomic contributions were not distinguished.

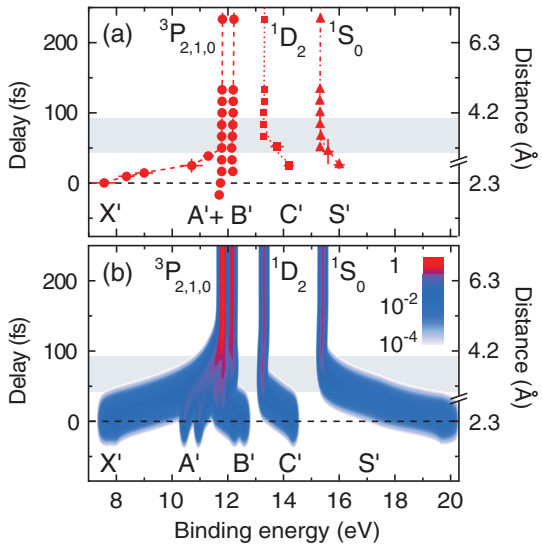

FIG. 3 (color). (a) Measured valence-electron binding energies versus delay and distance from the excited molecule (X'-S'), through a transition region (gray box) to the free atoms ($^3P_{2,1,0}$, $^1D_2$, $^1S_0$). Data points belonging to the same valence state are connected by lines. A selection of the data used to extract the delay or distance versus binding energy pairs is shown in Fig. 2. (b) Calculated binding energies and photoelectron intensities (logarithmic scale, color-coded intensity scale as indicated) for Fourier-transform-limited probe pulses (20 fs, 0.1 eV).

Delay time and internuclear distance can be related unambiguously [Fig. 3(a)] since the shape of the dissociative Br_2 $^1\Pi_u$ potential energy curve is known [6]. The dissociation time of 85 ± 15 fs corresponds to a nuclear distance of 3.8 ± 0.3 Å and hence to approximately $1.7R_e$ (equilibrium distance $R_e = 2.3$ Å for Br_2). We hence find a distance that is considerably shorter than $2R_e = 4.6$ Å, a criterion often used to define broken bonds. It is also much shorter than the ~5.5 Å, a distance where the dissociative potential energy curve becomes flat and, therefore, a distance that would be extracted from conventional laser femtochemistry experiments. Apparently, the electronic structure of the free atom is already established after 85 fs (at 3.8 Å), but it is perturbed out to ~160 fs (to ~5.5 Å) by the presence of the other nearby atom, causing small shifts of the potential energy. It is important to take this difference between the evolution of the electronic structure and the total energy into account in future investigations: Transition states show up during chemical reactions because nuclei and valence electrons rearrange but the time window for characterizing the bonding of transition states is determined by the evolution of the electronic structure and our results indicate that this window is smaller than anticipated.

The delay- or distance-versus-energy map in Fig. 3(a) depicts how the atomic $^1D_2$ and $^1S_0$ peaks arise from the C' ($^2\Pi_{u\frac{3}{2},\frac{1}{2}}$) and S' ($^2\Pi_{g\frac{3}{2},\frac{1}{2}}$, $^2\Pi_{u\frac{3}{2},\frac{1}{2}}$) final states of the excited molecule as the result of a shift by several eV to smaller binding energies during the first 50–70 fs. The $^3P_{2,1,0}$ multiplet arises from the X' ($^2\Pi_{g\frac{3}{2},\frac{1}{2}}$) state merging from lower energies with A' ($^2\Sigma_u$) and B' ($^2\Sigma_g$) after ~50 fs (final ionic states in brackets). The X' state is due to photoionization from the antibonding $8\sigma_u$ orbital populated by absorption of the pump photon. Its binding energy shift of −3.1 eV at 0 fs with respect to the X state of the ground-state molecule corresponds to the excitation energy. The states due to photoionization from σ orbitals (X', C', and S') show the largest binding energy shifts since they arise from atomic orbitals oriented along the bond whose overlap changes most considerably with increasing bond length. They shift so fast that even with transform-limited pulses [calculation in Fig. 3(b)] they would not show up as peaks in the spectrum as suggested in [6,7] but merely as broad intensity distributions as observed here. We find that the well-defined energy levels of the excited molecule do not exist any more after 50 ± 15 fs. Our observations therefore motivate an electronic-structure-based definition of a transition period from the molecular states of Br_2^* to the atomic states of Br starting 50 ± 15 fs after excitation (at 3.1 ± 0.3 Å) and lasting for 35 fs until the electronic structure of the free atom is established

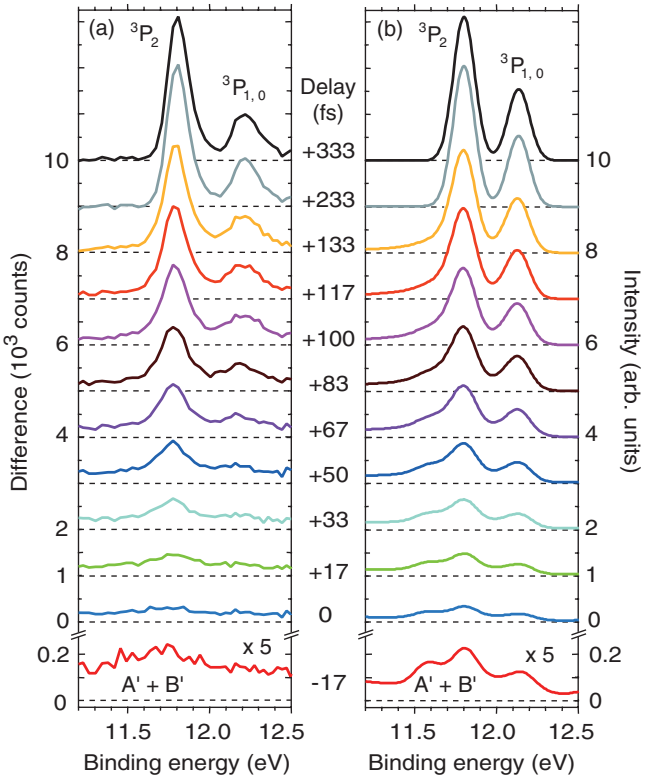

FIG. 4 (color). (a) Measured difference spectra and (b) calculated spectra for the ^3P binding energy region at indicated delays. Calculated spectra are based on the data in Fig. 3 including in addition the 120 fs duration of our probe pulses. The calculated spectrum at +333 fs was matched in intensity to the measured one; all other calculated spectra are displayed with respect to this.

after 85 fs (at 3.8 Å). It is during this transition period where the system appears to be intermediate between atoms and molecules that the valence electrons rearrange to form the orbitals of the free atom.

The evolution from the excited molecule with a broad spectrum to the free atom with atomic multiplet structure is shown for ^3P for all measured delays in Fig. 4(a). We find good overall agreement with the calculated spectra in Fig. 4(b), but calculated spin-orbit splitting and relative intensities in the atomic spectrum are not fully reproduced. Although the agreement of relative intensities is better than from pure LS coupling (5:4 for $^3P_2$:$^3P_{1,0}$), this discrepancy calls for an improved theoretical treatment of intensities by including the continuum wave functions of the photoionized electrons and, possibly, quantum dynamical MD simulations.

In conclusion, we mapped how the electrons that form a bond rearrange as the bond breaks. We observe how the valence states of photoexcited Br_2^* molecules evolve through a transition period to the photoelectron multiplet structure of free Br atoms. By probing the entire valence electronic structure we can unambiguously determine when the bond is broken. Our results and methodology provide a benchmark for future calculations and experiments using time-resolved photoelectron and x-ray emission spectroscopies to map the evolution of the valence electronic structure of molecules and atoms.

J. G. acknowledges support by the European Union Marie Curie program. M. O. acknowledges support from the Swedish research council and helpful discussions with H. Ågren and L. G. M. Pettersson.

*wernet@helmholtz-berlin.de
†Permanent address: European XFEL/DESY, Notkestrasse 85, D-22607 Hamburg, Germany.

[1] K. Sokolowski-Tinten *et al.*, Nature (London) **422**, 287 (2003).
[2] M. Bargheer *et al.*, Science **306**, 1771 (2004).
[3] S. L. Johnson *et al.*, Phys. Rev. Lett. **100**, 155501 (2008).
[4] C. Bressler *et al.*, Science **323**, 489 (2009).
[5] L. Nugent-Glandorf *et al.*, Phys. Rev. Lett. **87**, 193002 (2001).
[6] L. Nugent-Glandorf *et al.*, J. Chem. Phys. **117**, 6108 (2002).
[7] D. Strasser, F. Goulay, and S. R. Leone, J. Chem. Phys. **127**, 184305 (2007).
[8] E. Gagnon *et al.*, Science **317**, 1374 (2007).
[9] Z.-H. Loh and S. R. Leone, J. Chem. Phys. **128**, 204302 (2008).
[10] M. Meyer *et al.*, Phys. Rev. Lett. **101**, 193002 (2008).
[11] M. Bauer *et al.*, Phys. Rev. Lett. **87**, 025501 (2001).
[12] K. Read *et al.*, J. Appl. Phys. **90**, 294 (2001).
[13] P. Siffalovic, M. Drescher, and U. Heinzmann, Europhys. Lett. **60**, 924 (2002).
[14] A. Cavalleri *et al.*, Phys. Rev. Lett. **95**, 067405 (2005).
[15] A. M. Lindenberg *et al.*, Science **308**, 392 (2005).
[16] C. Stamm *et al.*, Nature Mater. **6**, 740 (2007).
[17] M. Shapiro, M. J. J. Vrakking, and A. Stolow, J. Chem. Phys. **110**, 2465 (1999).
[18] K. Ueda *et al.*, Phys. Rev. Lett. **83**, 3800 (1999).
[19] S. Hubinger and J. B. Nee, J. Photochem. Photobiol., A **86**, 1 (1995).
[20] R. J. Oldman, R. K. Sander, and K. R. Wilson, J. Chem. Phys. **63**, 4252 (1975).
[21] T. Pfeiffer, C. Spielmann, and G. Gerber, Rep. Prog. Phys. **69**, 443 (2006).
[22] Ph. Wernet *et al.*, Springer Ser. Chem. Phys. **88**, 45 (2007).
[23] See EPAPS Document No. E-PRLTAO-103-061927 for experimental details, details on data analysis, and details on the theory. For more information on EPAPS, see http://www.aip.org/pubservs/epaps.html.
[24] K. Andersson *et al.*, computer code P.-O. MOLCAS version 5.4, University of Lund, 2002.
[25] T. E. Glover *et al.*, Phys. Rev. Lett. **76**, 2468 (1996).
[26] J. L. Krause, M. Shapiro, and R. Bersohn, J. Chem. Phys. **94**, 5499 (1991).
[27] K. Kimura, T. Yamazaki, and Y. Achiba, Chem. Phys. Lett. **58**, 104 (1978).